Drude weight and total optical weight in a t - t' - J model

1996 J. Phys.: Condens. Matter 8 5089

(http://iopscience.iop.org/0953-8984/8/27/017)

J. Phys.: Condens. Matter **8** (1996) 5089–5100. Printed in the UK

Drude weight and total optical weight in a t–t'–J model

Gregory C Psaltakis

Department of Physics, University of Crete, and Research Centre of Crete, Heraklion, GR-71003, Greece

Received 31 October 1995

Abstract. We study the Drude weight D and the total optical weight K for a t–t'–J model on a square lattice that exhibits a metallic phase-modulated antiferromagnetic ground state close to half-filling. Within a suitable $1/N$ expansion that includes leading quantum-fluctuation effects, D and K are found to increase linearly with small hole doping away from the Mott metal–insulator transition point at half-filling. The slow zero-sound velocity near the latter transition identifies with the velocity of the lower-energy branch of the twofold excitation spectrum. At higher doping values, D and K eventually saturate and then start to decrease. These features are in qualitative agreement with optical conductivity measurements in doped antiferromagnets.

1. Introduction

The optical properties of the metallic state that emerges upon doping the insulating Heisenberg antiferromagnet with mobile holes are of great interest because such a system, currently described by a t–t'–J model, is believed to capture the low-energy physics of the high-T_c superconducting copper oxide layers [1]. In the context of the latter model we have recently calculated [2], using a suitable $1/N$ expansion, the real part of the finite-frequency optical conductivity, i.e., the optical absorption $\sigma(\omega)$, and found that its magnitude scales with low hole concentration while its low-frequency line shape displays a structureless broad-band regime. These results are in qualitative agreement with the generic properties of the midinfrared band observed in optical conductivity measurements [3–5] in doped antiferromagnets. Here we extend our earlier work [2] by presenting results for the Drude weight D and the total optical weight K that determine the zero-frequency response of the system and the optical conductivity sum rule, respectively. As is well known [6], the Drude weight D serves as an order parameter for the Mott metal–insulator transition occurring in such a system, hence the significance of its dependence on hole concentration and relevant coupling constants. Furthermore, the fraction of the total optical weight residing at zero frequency, i.e., the fraction D/K, defines the inverse of the mass enhancement factor. The latter quantity is a direct measure of the strength of the quasiparticle interactions or equivalently, in the context of the $1/N$ expansion, of the strength of the quantum fluctuations.

The t–t'–J model Hamiltonian can be expressed in terms of the Hubbard operators $\chi^{ab} = |a\rangle\langle b|$ as

$$H = -\sum_{i,j} t_{ij}\chi_i^{0\mu}\chi_j^{\mu 0} + \tfrac{1}{2}J\sum_{\langle i,j\rangle}(\chi_i^{\mu\nu}\chi_j^{\nu\mu} - \chi_i^{\mu\mu}\chi_j^{\nu\nu}) \tag{1}$$

where the index 0 corresponds to a hole, the Greek indices $\mu, \nu, \ldots$ assume two distinct values, for a spin-up and a spin-down electron, and the summation convention is invoked.

0953-8984/96/275089+12$19.50

Here J is the antiferromagnetic spin-exchange interaction between nearest-neighbour sites $\langle i, j\rangle$ on a square lattice, while for the hopping matrix elements t_{ij} we assume

$$t_{ij} = \begin{cases} t & \text{if } i, j \text{ are nearest neighbours} \\ -t' & \text{if } i, j \text{ are next-nearest neighbours} \\ 0 & \text{otherwise.} \end{cases} \tag{2}$$

Our conventions in (2) incorporate opposite signs for t and t' as dictated by quantum chemistry calculations [7, 8] for Cu–O clusters and fits of the shape of the Fermi surface observed by angle-resolved photoemission spectroscopy [9]. In [10] we generalized the local constraint associated with (1) to $\chi_i^{00} + \chi_i^{\mu\mu} = N$, where N is an arbitrary integer, and simplified the commutation properties of the χ^{ab}s to be those of the generators of the U(3) algebra. A generalized Holstein–Primakoff realization of this algebra in terms of Bose operators can then be employed to develop a perturbation theory based on the $1/N$ expansion, restoring the relevant physical value $N = 1$ at the end of the calculation. For an average electronic density n_e close to half-filling ($n_e \lesssim 1$) and a sufficiently large t', the ground state of (1) in the large-N limit is an unconventional metallic antiferromagnetic (AF) state characterized by the usual (π, π) modulation of the spin configuration and an unusual $(\pi, -\pi)$ phase modulation of the condensate [10]. It is the optical properties of this phase-modulated AF state that the present work is concerned with.

The remainder of this paper is organized as follows. Section 2 contains a brief summary of the relevant Kubo formalism for the optical conductivity. In section 3 we derive the analytic expressions of the $1/N$ expansion for the Drude weight and the total optical weight, including leading quantum-fluctuation effects. In section 4 we present explicit numerical results for the latter quantities along with some further comments on the optical absorption and a discussion of the zero-sound velocity which is related to the Drude weight and the inverse compressibility. Our conclusions are summarized in section 5.

2. Kubo formalism

Using standard linear-response theory, the Kubo formula for the real part of the frequency-dependent optical conductivity $\tilde{\sigma}(\omega)$ at zero temperature is expressed as the sum of two physically distinct terms [11, 12]:

$$\mathrm{Re}[\tilde{\sigma}(\omega)] = \pi e^2 D\delta(\omega) + \sigma(\omega). \tag{3}$$

The first term in (3), involving the delta function at zero frequency ($\omega = 0$), is due to the free acceleration of the charge-carrying mass by the electric field and therefore the associated spectral weight, i.e., the Drude weight D, should vanish in the insulating state and be finite in the metallic state [6]. D measures the ratio of the density of the mobile charge carriers to their mass. The second term in (3), called the optical absorption $\sigma(\omega)$, is due to finite-frequency ($\omega > 0$) optical transitions to excited quasiparticle states. More explicitly we have that

$$\sigma(\omega) = \frac{\pi}{\omega\Lambda} \sum_{m\neq 0} |\langle m|J|0\rangle|^2 \delta[(E_m - E_0) - \omega] \tag{4}$$

where the summation is taken over a complete set of energy eigenstates $|m\rangle$ with excitation energies $(E_m - E_0)$ above the ground state $|0\rangle$, Λ is the total number of lattice sites, and J is one of the Cartesian components of the current operator $\boldsymbol{J}$ associated with (1),

$$\boldsymbol{J} = \mathrm{i}e \sum_{i,j} t_{ij}(\boldsymbol{R}_i - \boldsymbol{R}_j)\chi_i^{0\mu}\chi_j^{\mu 0} \tag{5}$$

where $\boldsymbol{R}_i$ is the position vector for site i. Similarly, the Drude weight D is given by

$$D = K - \frac{2}{e^2 \Lambda} \sum_{m \neq 0} \frac{|\langle m|J|0\rangle|^2}{E_m - E_0} \tag{6}$$

where K is the expectation value

$$K = \frac{2}{z\Lambda} \langle 0| -T|0\rangle \tag{7}$$

with the operator T defined as

$$T = -\sum_{i,j} t_{ij} |\boldsymbol{R}_i - \boldsymbol{R}_j|^2 \chi_i^{0\mu} \chi_j^{\mu 0} \tag{8}$$

where $z = 4$ is the coordination number of the square lattice. Integrating now, over frequency, both sides of (3), using the identity $\int_0^\infty \mathrm{d}\omega\ \delta(\omega) = \frac{1}{2}$ and the explicit forms (4) and (6), we arrive at the well-known optical conductivity sum rule [13]

$$\int_0^\infty \mathrm{d}\omega\ \mathrm{Re}[\tilde{\sigma}(\omega)] = \frac{\pi e^2}{2} K \tag{9}$$

which, indeed, identifies K as the total optical spectral weight.

It should be noted that in lattice models involving only nearest-neighbour hopping, T defined in (8) coincides with the kinetic energy operator given by the first term on the right-hand side of (1). However, the presence of an additional next-nearest-neighbour hopping, i.e., a hopping t' along the diagonal of the square unit cell as in the t–t'–J model under study, invalidates the latter simple result, noting that: $|\boldsymbol{R}_i - \boldsymbol{R}_j|^2 = 2$, for next-nearest-neighbour sites i, j. Therefore in this more general case, the total optical weight K given by (7) is *not* just the kinetic energy expectation value in the ground state. Nevertheless, by an elementary application of the Hellmann–Feynman theorem, K can still be extracted from the ground-state energy $\langle 0|H|0\rangle$ by differentiation with respect to the hoppings [14] t and t':

$$K = -\frac{2}{z\Lambda} \left(t \frac{\partial}{\partial t} + 2t' \frac{\partial}{\partial t'} \right) \langle 0|H|0\rangle . \tag{10}$$

The identity (10) is actually implemented in the following section to derive the leading terms of the $1/N$ expansion of K from the corresponding terms of $\langle 0|H|0\rangle$ which our theory readily provides.

3. $1/N$ expansion

The $1/N$ expansion of the Hamiltonian (1) and the optical absorption (4) around the phase-modulated AF configuration, up to and including terms of order N, has been carried out in our earlier work [10, 2]. For ease of reference, we quote in (11)–(14) the main results necessary for our present development. Specifically, the expansion of the Hamiltonian (1) reads [10]

$$H = N^2 \Lambda E_0 + N \Lambda E_1 + N \sum_{\boldsymbol{q}} \left[\omega_1(\boldsymbol{q}) A_{\boldsymbol{q}}^* A_{\boldsymbol{q}} + \omega_2(\boldsymbol{q}) B_{\boldsymbol{q}}^* B_{\boldsymbol{q}} \right] \tag{11}$$

where E_0 and E_1 are the classical (large-N limit) and zero-point energy per lattice site, respectively, for the relevant physical value $N = 1$:

$$\begin{aligned} E_0 &= -zt' n_e (1 - n_e) - \frac{zJ}{4} n_e^2 \\ E_1 &= -\frac{zt'}{2} (2 - n_e) - \frac{zJ}{4} n_e + \frac{1}{2\Lambda} \sum_{\boldsymbol{q}} [\omega_1(\boldsymbol{q}) + \omega_2(\boldsymbol{q})] . \end{aligned} \tag{12}$$

In the above A_q and B_q are the normal-mode operators that diagonalize the leading (quadratic) quantum fluctuations while $\omega_n(\boldsymbol{q})$, $n = 1, 2$, are the dispersions of the two branches of the spectrum of elementary excitations. An immediate consequence of (11) is the following result for the $1/N$ expansion of the ground-state energy, up to and including terms of order N:

$$\langle 0|H|0\rangle = N^2 \Lambda E_0 + N \Lambda E_1. \tag{13}$$

The corresponding expansion of the optical absorption (4) reads [2]

$$\sigma(\omega) = N \frac{2\pi(et)^2}{\omega \Lambda} \sum_{\boldsymbol{q}} u^2(\boldsymbol{q}) \delta[\omega_1(\boldsymbol{q}) + \omega_2(\boldsymbol{q}) - \omega]. \tag{14}$$

The analytic expressions for the dimensionless function $u^2(\boldsymbol{q})$, corresponding to the current matrix elements, and the dispersions $\omega_n(\boldsymbol{q})$, $n = 1, 2$, are rather involved and are summarized in the appendix. The result (14) has been extensively discussed in our earlier work [2] while some further comments are added in section 4.

At present, an important point to note in (14) is the lack of a classical contribution, i.e., a term of order N^2, to $\sigma(\omega)$. In other words, the finite-frequency component $\sigma(\omega)$ of the optical conductivity is due *exclusively* to the quantum fluctuations whose leading contribution, within the present $1/N$ expansion scheme, is of order N. This conclusion is consistent with similar observations made by Bang and Kotliar [15] for the finite-frequency optical conductivity of the simple t–J model treated by a slave-boson diagrammatic $1/N$ expansion technique.

The derivation of the $1/N$ expansion of the Drude weight D and the total optical weight K, up to and including terms of order N, proceeds now in two steps: (i) the result (13) is used to implement identity (10); and (ii) the second term on the right-hand side of (6) is expressed initially as the integral of (4) over positive frequencies and then (14) is exploited to obtain immediately its $1/N$ expansion. Taking into account (12), the final analytic results of this straightforward procedure may be written in the form

$$D = N^2 D_0 + N D_1 \tag{15}$$

$$K = N^2 K_0 + N K_1 \tag{16}$$

where D_0 and K_0 are the classical (large-N limit) contributions to the Drude weight and the total optical weight, respectively:

$$D_0 = K_0 = -\frac{2}{z}\left(t\frac{\partial}{\partial t} + 2t'\frac{\partial}{\partial t'}\right)E_0 = 4t' n_e(1 - n_e) \tag{17}$$

while D_1 and K_1 are the corresponding contributions due to leading quantum-fluctuation effects:

$$K_1 = -\frac{2}{z}\left(t\frac{\partial}{\partial t} + 2t'\frac{\partial}{\partial t'}\right)E_1 \tag{18}$$

$$D_1 = K_1 - \frac{4t^2}{\Lambda}\sum_{\boldsymbol{q}} \frac{u^2(\boldsymbol{q})}{\omega_1(\boldsymbol{q}) + \omega_2(\boldsymbol{q})}. \tag{19}$$

The equality $D_0 = K_0$ quoted in (17) is a consequence of the absence of quantum fluctuations in the large-N limit and implies that in this classical approximation, described by the terms of order N^2, the δ-function Drude peak centred at zero frequency ($\omega = 0$) carries the total optical weight. However, as noted earlier on, the leading quantum fluctuations, described by the terms of order N, already give rise to optical absorption and hence distribute part of the total optical weight to finite frequencies ($\omega > 0$). The presence of the terms

of order N in (15) and (16) leads therefore to $D < K$; a generic property anticipated also from (6) and (19).

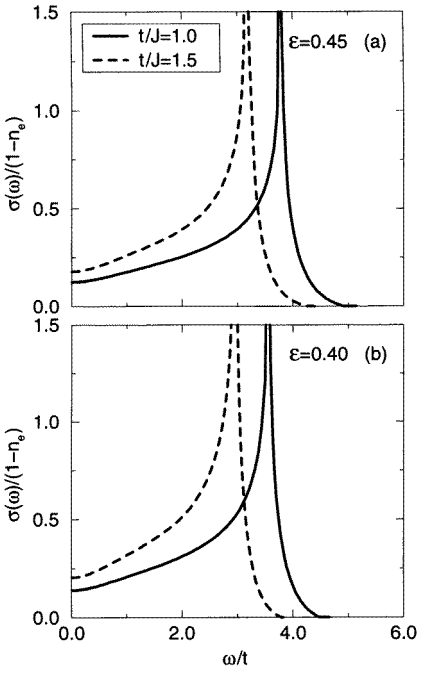

Figure 1. Optical absorption $\sigma(\omega)$ (in units of $e^2/\hbar$) over hole concentration $(1-n_e)$ versus frequency for $1-n_e = 0.10$, $t/J = 1.0$ (solid line) or $t/J = 1.5$ (dashed line), and (a) $\varepsilon = 0.45$, (b) $\varepsilon = 0.40$.

In view of (12) and the explicit forms quoted in the appendix, the derivatives with respect to t and t' appearing in (18) can be carried out analytically. The remaining wave-vector integrations over the square Brillouin zone in (18) and (19), as well as in (14), can then be performed numerically. Explicit numerical results derived from (15)–(19) in the way just described are presented in the following section.

4. Explicit results

For completeness and better insight into the results for the Drude weight and the total optical weight that will be presented shortly, it is instructive to begin our discussion here with some examples of the optical absorption line shape $\sigma(\omega)$. In figure 1 we show $\sigma(\omega)$, determined from (14) with $N = 1$, for typical values of the dimensionless ratios $\varepsilon = t'/t$, t/J and the hole concentration $(1-n_e)$ that are relevant for the copper oxide layers [7, 8, 9]. As noted in [2], the limiting value $\sigma(\omega \to 0)$ is finite, at finite hole doping, while for small doping values (such as the 10% hole doping considered in figure 1) the high-frequency divergence of $\sigma(\omega)$ comes from the $\boldsymbol{q} = (\pi/2, \pi/2)$ point of the Brillouin zone. The frequency position of this peak (divergence) is then determined as

$$[\omega_1(\boldsymbol{q}) + \omega_2(\boldsymbol{q})]_{\boldsymbol{q}=(\pi/2,\pi/2)} = zt'(2-n_e) + \frac{zJ}{2}n_e \tag{20}$$

and apparently is independent of the nearest-neighbour hopping t. For the parameter values corresponding to the solid line of figure 1(a), the peak position of $\sigma(\omega)$ calculated from (20) is given by $\omega = 3.78J$. The latter value, with an estimated [16–18] $J \approx 0.13$–0.16 eV, accounts aptly for the $\omega \approx 0.5$ eV peak of the midinfrared band observed in optical conductivity measurements [3, 4, 5] in doped antiferromagnets.

From the explicit form (20) it follows that close to half-filling and for parameters satisfying $2t\varepsilon/J < 1$ the peak of $\sigma(\omega)$ shifts slowly to lower frequencies upon hole doping, i.e., with increasing $(1-n_e)$. Such a systematic shift of the peak of the midinfrared band is, indeed, observed in the aforementioned optical conductivity measurements. Interestingly enough, close to half-filling the same condition $2t\varepsilon/J < 1$ has been shown in [10] to ensure the softening of the magnon velocity upon hole doping—a trend that is also observed in inelastic neutron scattering measurements from doped antiferromagnets [16, 17]. The present theory provides therefore a context for the qualitative understanding of both experimental observations. Concluding our comments on $\sigma(\omega)$ we note that (3) and (9) yield $\int_0^\infty d\omega\, \sigma(\omega) = (\pi e^2/2)(K - D)$. Therefore, the spectral weight carried by the finite-frequency component $\sigma(\omega)$ is given by the difference $K - D$, and hence its dependence on the parameters ε, t/J, and n_e follows from that of D and K.

Let us now consider the large-N limit contributions D_0 and K_0 to the Drude weight and the total optical weight, respectively. The equality of these two quantities has already been discussed following (19). Here we note that the vanishing overlap between the opposite sublattice spin states in the AF configuration, along with the absence of quantum fluctuations in the large-N limit, leaves the direct hopping t' between same sublattice sites as the only relevant process of charge transport in this classical approximation. This argument makes plausible the independence of D_0, K_0 from t and J seen in (17).

Furthermore, the n_e-dependence in (17) implies that: (i) $D_0 = K_0 \propto n_e$, for $n_e \to 0$; and (ii) $D_0 = K_0 \propto (1 - n_e)$, for $n_e \to 1$. The linear increase of D_0 and K_0 with small electron density n_e away from the empty-lattice limit ($n_e = 0$) is, of course, an expected behaviour in this 'free'-electron gas regime. On the other hand, the linear increase of D_0 and K_0 with small hole concentration $(1-n_e)$ away from the half-filled-band limit ($n_e = 1$) is an important consequence of the local constraint which prohibits the occupancy of any lattice site by more than one electron and leads inevitably to the Mott insulator at half-filling ($D_0 = 0 = K_0$, for $n_e = 1$). The latter property, typified in point (ii) above, serves to interpret the 'free' charge carriers near half-filling as being holes rather than electrons. Then, the position of the maximum of D_0 located at quarter-filling ($n_e = \frac{1}{2}$) provides an estimate of the critical amount of doping at which the character of the charge carriers changes from holelike to electronlike with increasing $(1 - n_e)$. The present large-N limit results already capture generic features of the n_e-dependence of the Drude weight and the total optical weight that are derived by exact diagonalization of the simple t–J model and the large-U Hubbard model on small clusters [19, 20, 1]. The reason can be traced to the fact that our generalized Holstein–Primakoff realization [10] resolves explicitly the local constraint, and thus the ensuing $1/N$ expansion incorporates already part of the strong-correlation effects, implied by this constraint, in the leading order.

As a check of consistency of the quantum-liquid description emerging from the present $1/N$ expansion scheme it is worthwhile at this point to discuss briefly the zero-sound velocity, i.e., the velocity of the long-wavelength charge excitations, in the physically relevant regime near half-filling ($n_e \to 1$). As demonstrated in detail in [10], a separation of spin and charge degrees of freedom sets in progressively and becomes *asymptotically* exact as the half-filled-band limit is approached. The latter limit permits then an accurate classification of the elementary excitations in terms of a mode that describes the spin

excitations and a mode that describes the charge excitations. At long wavelengths ($|\boldsymbol{q}| \to 0$), in particular, the latter mode corresponds to the lower-energy branch of the twofold excitation spectrum given by $\omega_2(\boldsymbol{q}) = c_2|\boldsymbol{q}|$. Thus near half-filling ($n_e \to 1$) the velocity of the long-wavelength charge excitations is given by c_2. On the other hand, in the context of conventional quantum-liquid theory [21] the zero-sound velocity may be expressed in terms of the Drude weight D_0 and the inverse compressibility $1/\kappa = n_e^2 E_0''$, where $E_0'' = \partial^2 E_0/\partial n_e^2$, as $\sqrt{D_0/(n_e^2\kappa)} = \sqrt{D_0 E_0''}$. Hence the consistency of the quantum-liquid description requires the validity of the identity $c_2 = \sqrt{D_0 E_0''}$, for $n_e \to 1$. The asymptotic form of c_2 for $n_e \to 1$ has been derived in [10] by considering explicitly the long-wavelength limit of $\omega_2(\boldsymbol{q})$. Here, using (12) and (17) to calculate $\sqrt{D_0 E_0''}$ and comparing with the latter result for c_2, one can easily verify that indeed [22]

$$c_2 = \sqrt{D_0 E_0''} = 2\varepsilon\left[2ztJ\left(\frac{t}{J} - \frac{1}{4\varepsilon}\right)(1-n_e)\right]^{1/2} \qquad \text{for } n_e \to 1. \tag{21}$$

In view of the radically different way in which c_2 and $\sqrt{D_0 E_0''}$ are derived, the relation (21) provides a stringent consistency check of our theory and serves to identify unambiguously c_2 as the slow zero-sound velocity for $n_e \to 1$. Furthermore, from (12) it follows that E_0'' is independent of n_e. Hence (21) reveals that the physical reason for the softening of the velocity c_2 of the lower-energy branch ω_2 near the Mott metal–insulator transition at half-filling ($c_2 \propto \sqrt{1-n_e} \to 0$, for $n_e \to 1$) is the collapse of the Drude weight, which in turn is a direct consequence of the local constraint. It should be noted that this slow zero-sound mode near the Mott transition appears also in slave-boson treatments of the local constraint when the fluctuations of the associated statistical gauge field are taken into account beyond the mean-field approximation [23]. Concluding our discussion of the zero-sound velocity we note that away from the asymptotic regime $n_e \to 1$ and with increasing hole concentration, ω_2 (as well as ω_1) involves an increasingly strong hybridization between spin and charge degrees of freedom, and consequently c_2 no longer corresponds to the velocity of the long-wavelength charge excitations.

Having analysed the classical (large-N limit) contributions to the Drude weight and the total optical weight, we consider in the remainder of this section the complete results for D and K that include the leading quantum-fluctuation corrections, as determined from (15) and (16), respectively, with $N = 1$. In figure 2 (for $\varepsilon = 0.45$) and figure 3 (for $\varepsilon = 0.40$) we draw as a function of the hole concentration $(1-n_e)$: (a) the Drude weight D, (b) the total optical weight K, and (c) the fraction D/K, for $t/J = 1.0$ (solid line) or $t/J = 1.5$ (dashed line). For comparison, in each figure we also depict by a dotted line the classical (large-N limit) result for the quantity shown: (a) D_0, (b) K_0, and (c) D_0/K_0. We recall that the latter classical results, determined from (17), are independent of the ratio t/J. Our main observations from figure 2 and figure 3 are summarized as follows.

(i) D and K increase linearly with small hole concentration $(1-n_e)$ away from the Mott metal–insulator transition point at half-filling ($n_e = 1$), consistent with the notion that the 'free' charge carriers in this regime are the holes. However, as a result of the leading quantum fluctuations, D and K are no longer equal. Close to half-filling and for the typical values of ε and t/J considered, the fraction D/K is reduced from its 'classical' value of 1 to about 0.5 and is almost independent of $(1-n_e)$ in the doping range of interest; see the solid and dashed lines in figure 2(c) and figure 3(c). These results are consistent with optical conductivity measurements [3–5] in doped antiferromagnets. In particular, for $\varepsilon = 0.45$, $t/J = 1.0$, corresponding to the solid line of figure 2(c), and a typical 10% hole doping we have: $D/K = 0.52$, corresponding to a mass enhancement factor $K/D = 1.92$. The

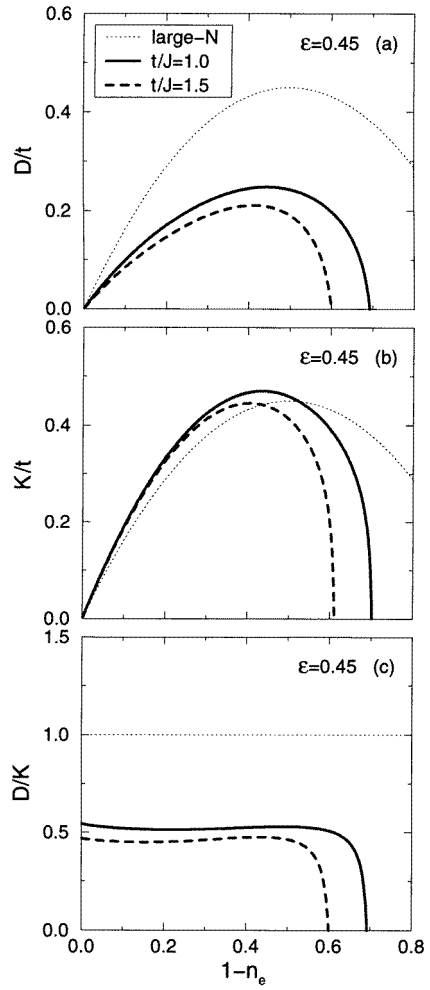

Figure 2. For $\varepsilon = 0.45$ and $t/J = 1.0$ (solid line) or $t/J = 1.5$ (dashed line), including leading quantum-fluctuation effects: (a) Drude weight D versus hole concentration. (b) Total optical weight K versus hole concentration. (c) Fraction D/K versus hole concentration. In each figure, the dotted line is the classical (large-N limit) result for the quantity shown and is independent of t/J according to equation (17).

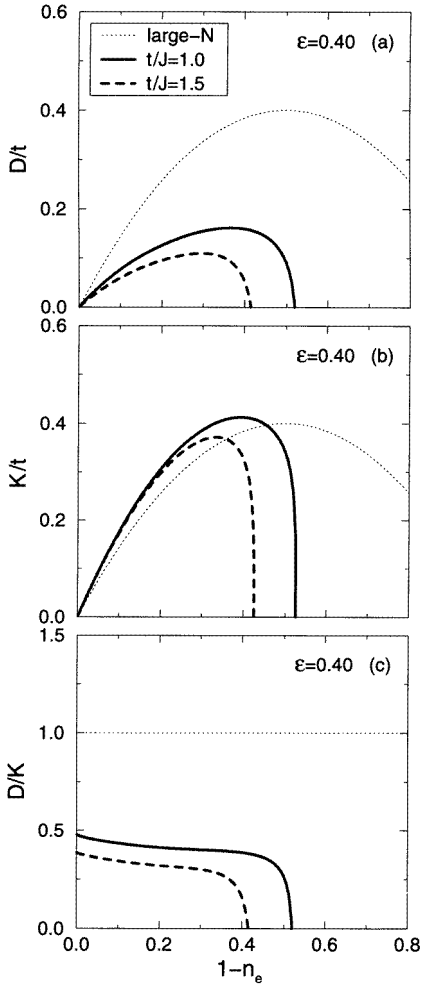

Figure 3. For $\varepsilon = 0.40$ and $t/J = 1.0$ (solid line) or $t/J = 1.5$ (dashed line), including leading quantum-fluctuation effects: (a) Drude weight D versus hole concentration. (b) Total optical weight K versus hole concentration. (c) Fraction D/K versus hole concentration. In each figure, the dotted line is the classical (large-N limit) result for the quantity shown and is independent of t/J according to equation (17).

latter value compares reasonably well with the experimental estimate [4] $(K/D)_{\rm exp} \approx 2.3$. Furthermore, our typical value $D/K = 0.52$ is compatible with the corresponding prediction of 0.6 derived by exact diagonalization [20] and anyon techniques [24] for the simple t–J model, and implies that 52% of the total optical weight resides at the zero-frequency Drude peak $\pi e^2 D\delta(\omega)$ while the rest is carried by the finite-frequency component $\sigma(\omega)$. It should be noted that the strength of the quasiparticle interactions, as inferred from the mass enhancement factor $K/D \approx 2.0$, is not exceptionally large [4]. This fact, however, is not surprising noting that important correlation effects, implied by the local constraint, are

already absorbed into the charge carrier density which near half-filling is given by the hole concentration $1-n_e$ that vanishes at $n_e=1$, leading to the Mott metal–insulator transition.

(ii) At higher doping values, D and K eventually saturate and then start to decrease. However, the leading quantum fluctuations shift the maximum of D and K away from its 'classical' location at quarter-filling towards half-filling. This shift is small and slightly different for D and K. As noted earlier on and emphasized by Dagotto *et al* [20], the position of the maximum of D provides an estimate of the doping value at which the charge carriers change from holelike to electronlike with increasing $(1-n_e)$; hence at roughly the same position the Hall coefficient R_H should change sign from positive to negative. For $\varepsilon=0.45$ (0.40) and $t/J=1.0$, corresponding to the solid line of figure 2(a) (figure 3(a)), the maximum of D occurs at the hole concentration $1-n_e=0.44$ (0.36). The latter result is then compatible with numerical and analytical calculations [25] of R_H, in the context of the simple t–J model, that predict a sign change at a hole concentration of about 0.40–0.33, and with Hall effect measurements [26] in doped antiferromagnets that report a sign change of R_H at a hole concentration of about 0.3.

(iii) We cannot approach the 'free'-electron gas regime close to the empty-lattice limit ($n_e=0$), because the phase-modulated AF configuration, around which the present $1/N$ expansion is carried out, becomes unstable beyond a critical value of the hole concentration $(1-n_e)$. The intervening instability is reflected in the elementary excitations whereby the velocity c_2 of the lower-energy branch ω_2 becomes zero at the critical doping value [10]. This results in a very rapid decrease of D, K, and D/K in the immediate neighbourhood of the latter doping value—a behaviour clearly seen in figure 2 and figure 3. In this critical doping regime, the magnitude of the (negative) leading quantum-fluctuation corrections D_1 and K_1 becomes even larger than that of the classical (large-N limit) terms D_0 and K_0, and therefore the $1/N$ expansion breaks down.

(iv) Finally, by comparing the solid and dashed lines in figure 2 and figure 3 we conclude that at any given doping value D, K, and D/K all increase with increasing t' and/or J. This trend is consistent with similar results derived by exact diagonalization of the t–J model, extended to include the so-called three-site term [19], and of the Hubbard model [20]. Therefore, this trend should be regarded as being generic for models involving a direct or an effective hopping between same sublattice sites.

5. Conclusions

In this paper we have presented a detailed study of the Drude weight D, the total optical weight K, and the fraction D/K that defines the inverse of the mass enhancement factor, in the phase-modulated AF state of the t–t'–J model (1), (2). The generic features of these quantities observed in optical conductivity measurements [3–5] in doped antiferromagnets are qualitatively reproduced when the leading quantum-fluctuation effects, around the aforementioned semiclassical ground state, are taken into account within a suitable $1/N$ expansion.

Specifically, D and K increase linearly with small hole doping away from the Mott metal–insulator transition at half-filling, consistent with the notion that the 'free' charge carriers in this regime are the holes. Our theoretical prediction of a mass enhancement factor $K/D\approx 2.0$ that is almost independent of the hole concentration, in the doping range of interest, compares reasonably well with the corresponding experimental estimate [4]. With increasing hole doping D (and K) eventually reaches a maximum at a value that is compatible with measurements [26] of the critical doping at which the Hall coefficient R_H changes sign from positive to negative, signalling a change in the character of the charge

carriers from holelike to electronlike. Furthermore, for typical parameter values the peak position (20) of the finite-frequency component $\sigma(\omega)$ of the optical conductivity accounts aptly for the experimentally observed 0.5 eV peak of the midinfrared band [3–5].

Finally, the slow zero-sound velocity near the Mott metal–insulator transition point at half-filling is shown to identify with the velocity of the lower-energy branch of the twofold excitation spectrum, thus providing a stringent consistency check of the quantum-liquid description emerging from the present $1/N$ expansion scheme.

Acknowledgments

I would like to thank N Papanicolaou for valuable discussions. This work was supported by Grant No CHRX-CT93-0332 from the EEC and Grant No 91EΔ631 from the Greek Secretariat for Research and Technology.

Appendix

In this appendix we summarize the analytic expressions for the dispersions $\omega_n(\boldsymbol{q})$, $n = 1, 2$, of the two branches of the spectrum of elementary excitations, and the dimensionless function $u^2(\boldsymbol{q})$, corresponding to the current matrix elements, that enter the optical absorption (14) and the leading quantum-fluctuation corrections (18), (19) for the Drude weight and the total optical weight.

Following the notation conventions of [10], the dispersions $\omega_n(\boldsymbol{q})$, $n = 1, 2$, are given by

$$\begin{aligned}\omega_1^2(\boldsymbol{q}) &= R(\boldsymbol{q}) + 2\sqrt{S(\boldsymbol{q})} \\ \omega_2^2(\boldsymbol{q}) &= R(\boldsymbol{q}) - 2\sqrt{S(\boldsymbol{q})}\end{aligned} \tag{A1}$$

with

$$R(\boldsymbol{q}) = \left[\omega_q^{(+)}\right]^2 + \left[\omega_q^{(-)}\right]^2 + \tau_q^2 - \lambda_q^2 - \left[\nu_q^{(+)}\right]^2 - \left[\nu_q^{(-)}\right]^2 \tag{A2}$$

and

$$S(\boldsymbol{q}) = \left[\omega_q^{(+)}\omega_q^{(-)} - \lambda_q\nu_q^{(-)}\right]^2 + \left[\omega_q^{(+)}\tau_q - \nu_q^{(+)}\lambda_q\right]^2 - \left[\omega_q^{(-)}\nu_q^{(+)} - \nu_q^{(-)}\tau_q\right]^2 \tag{A3}$$

where for an arbitrary wave vector $\boldsymbol{q} = (q_x, q_y)$ the explicit forms of the coefficients $\omega_q^{(\pm)}$, τ_q, λ_q, and $\nu_q^{(\pm)}$ read

$$\lambda_q = \frac{zt'}{4}\frac{n_e^2}{(1-n_e)}(1 - \cos q_x \cos q_y) + \frac{zt'}{2}n_e(1 + \cos q_x \cos q_y) \tag{A4}$$

$$\tau_q = \lambda_q - \frac{zJ}{4}n_e\left[1 + \frac{1}{2}(\cos q_x + \cos q_y)\right] \tag{A5}$$

$$\nu_q^{(+)} = \lambda_q - \frac{zJ}{4}n_e(\cos q_x + \cos q_y) \tag{A6}$$

$$\nu_q^{(-)} = \frac{zt}{4}n_e(\cos q_x - \cos q_y) \tag{A7}$$

$$\omega_q^{(+)} = \nu_q^{(+)} + \lambda_q - \tau_q + zt'(1-n_e)(1 - \cos q_x \cos q_y) \tag{A8}$$

$$\omega_q^{(-)} = \nu_q^{(-)} - \frac{zt}{2}(1-n_e)(\cos q_x - \cos q_y). \tag{A9}$$

The analytic expression for the function $u^2(\boldsymbol{q})$ is very involved. However, the result can be presented in a compact manner with the help of a four-component matrix notation

[10]. To this end we introduce the 4×4 matrices ρ_1, ρ_2, and ρ_3, defined as $\rho_i = \sigma_i \otimes 1$, $i = 1, 2, 3$, with the σ_i denoting the ordinary 2×2 Pauli matrices. The same symbols σ_i will also be used in the following to denote the 4×4 matrices $1 \otimes \sigma_i$, $i = 1, 2, 3$, for notational simplicity. We then have

$$u^2(\boldsymbol{q}) = \tfrac{1}{2}[u_x^2(\boldsymbol{q}) + u_y^2(\boldsymbol{q})] \tag{A10}$$

where $u_\alpha^2(\boldsymbol{q})$, $\alpha = x, y$, are positive-definite dimensionless functions expressed as traces over 4×4 matrices. Specifically,

$$u_\alpha^2(\boldsymbol{q}) = -\left(\frac{1}{4}\right)^2 \frac{1}{\omega_1(\boldsymbol{q})\omega_2(\boldsymbol{q})S(\boldsymbol{q})}\big\{\mathrm{Tr}[v_\alpha(\boldsymbol{q})A(\boldsymbol{q}, \omega_1(\boldsymbol{q}))v_\alpha(\boldsymbol{q})A(\boldsymbol{q}, -\omega_2(\boldsymbol{q}))] + \mathrm{Tr}[v_\alpha(\boldsymbol{q})A(\boldsymbol{q}, \omega_2(\boldsymbol{q}))v_\alpha(\boldsymbol{q})A(\boldsymbol{q}, -\omega_1(\boldsymbol{q}))]\big\} \tag{A11}$$

where $v_\alpha(\boldsymbol{q})$, $\alpha = x, y$, and $A(\boldsymbol{q}, \omega)$ are the 4×4 real matrices defined below:

$$v_x(\boldsymbol{q}) = \sin q_x\left[-\varepsilon\left(1 - \frac{3n_e}{2}\right)\cos q_y - \frac{1}{2}\left(1 - \frac{3n_e}{2}\right)\sigma_3 + \frac{\varepsilon}{2}n_e \cos q_y \sigma_1 + \frac{\mathrm{i}}{4}n_e\rho_1\sigma_2\right] \tag{A12}$$

$$v_y(\boldsymbol{q}) = \sin q_y\left[-\varepsilon\left(1 - \frac{3n_e}{2}\right)\cos q_x + \frac{1}{2}\left(1 - \frac{3n_e}{2}\right)\sigma_3 + \frac{\varepsilon}{2}n_e \cos q_x \sigma_1 - \frac{\mathrm{i}}{4}n_e\rho_1\sigma_2\right] \tag{A13}$$

$$A(\boldsymbol{q}, \omega) = [\omega + \mathcal{H}(\boldsymbol{q})][\omega^2 - R(\boldsymbol{q}) + 2\mathcal{M}(\boldsymbol{q})] \tag{A14}$$

with

$$\mathcal{H}(\boldsymbol{q}) = \omega_{\boldsymbol{q}}^{(+)}\rho_3 + \omega_{\boldsymbol{q}}^{(-)}\rho_3\sigma_3 + \tau_{\boldsymbol{q}}\rho_3\sigma_1 + \mathrm{i}\lambda_{\boldsymbol{q}}\rho_2 + \mathrm{i}\nu_{\boldsymbol{q}}^{(+)}\rho_2\sigma_1 + \mathrm{i}\nu_{\boldsymbol{q}}^{(-)}\rho_2\sigma_3 \tag{A15}$$

and

$$\mathcal{M}(\boldsymbol{q}) = \left[\omega_{\boldsymbol{q}}^{(+)}\omega_{\boldsymbol{q}}^{(-)} - \lambda_{\boldsymbol{q}}\nu_{\boldsymbol{q}}^{(-)}\right]\sigma_3 + \left[\omega_{\boldsymbol{q}}^{(+)}\tau_{\boldsymbol{q}} - \nu_{\boldsymbol{q}}^{(+)}\lambda_{\boldsymbol{q}}\right]\sigma_1 + \mathrm{i}\left[\omega_{\boldsymbol{q}}^{(-)}\nu_{\boldsymbol{q}}^{(+)} - \nu_{\boldsymbol{q}}^{(-)}\tau_{\boldsymbol{q}}\right]\rho_1\sigma_2. \tag{A16}$$

In conclusion it is worth emphasizing that the dispersions $\omega_n(\boldsymbol{q})$, $n = 1, 2$, defined in (A1), as well as the function $u^2(\boldsymbol{q})$ defined in (A10), depend on $\boldsymbol{q}$ only through the factors $\cos q_x$ and $\cos q_y$ and are symmetric under the interchange of variables (q_x, q_y): $\omega_n(q_x, q_y) = \omega_n(q_y, q_x)$, $n = 1, 2$, and $u^2(q_x, q_y) = u^2(q_y, q_x)$.

References

[1] For a recent review, see
Dagotto E 1994 *Rev. Mod. Phys.* **66** 763
[2] Psaltakis G C 1995 *Phys. Rev.* B **51** 2979
[3] Cooper S L *et al* 1990 *Phys. Rev.* B **41** 11 605
[4] Orenstein J *et al* 1990 *Phys. Rev.* B **42** 6342
[5] Uchida S *et al* 1991 *Phys. Rev.* B **43** 7942
[6] Kohn W 1964 *Phys. Rev.* **133** A171
[7] Hybertsen M S, Stechel E B, Schluter M and Jennison D R 1990 *Phys. Rev.* B **41** 11 068
[8] Sawatzky G A 1990 *Earlier and Recent Aspects of Superconductivity* ed J G Bednorz and K A Müller (Berlin: Springer) p 345
[9] Yu J and Freeman A J 1991 *J. Phys. Chem. Solids* **52** 1351
[10] Psaltakis G C and Papanicolaou N 1993 *Phys. Rev.* B **48** 456
[11] Shastry B S and Sutherland B 1990 *Phys. Rev. Lett.* **65** 243
Shastry B S 1992 *Mod. Phys. Lett.* B **6** 1427
[12] Scalapino D J, White S R and Zhang S C 1992 *Phys. Rev. Lett.* **68** 2830; 1993 *Phys. Rev.* B **47** 7995
[13] Bari R A, Adler D and Lange R V 1970 *Phys. Rev.* B **2** 2898

Maldague P F 1977 *Phys. Rev.* B **16** 2437
Baeriswyl D, Gros C and Rice T M 1987 *Phys. Rev.* B **35** 8391
[14] Baeriswyl D, Carmelo J and Luther A 1986 *Phys. Rev.* B **33** 7247; 1986 *Phys. Rev.* B **34** 8976(E)
[15] Bang Y and Kotliar G 1993 *Phys. Rev.* B **48** 9898
[16] Aeppli G *et al* 1989 *Phys. Rev. Lett.* **62** 2052
[17] Rossat-Mignod J *et al* 1991 *Dynamics of Magnetic Fluctuations in High-Temperature Superconductors* ed G Reiter, P Horsch and G C Psaltakis (New York: Plenum) p 35
[18] Shamoto S *et al* 1993 *Phys. Rev.* B **48** 13 817
[19] Stephan W and Horsch P 1992 *Int. J. Mod. Phys.* B **6** 589
[20] Dagotto E *et al* 1992 *Phys. Rev.* B **45** 10 741
[21] Pines D and Nozières P 1989 *The Theory of Quantum Liquids* (New York: Addison-Wesley) vol I
[22] Note that an expression analogous to $\sqrt{D_0 E_0''}$ for the velocity of the long-wavelength charge excitations in the one-dimensional Hubbard model appears implicitly also in the work of
Schulz H J 1990 *Phys. Rev. Lett.* **64** 2831
[23] Rodriguez J P 1994 *Phys. Rev. Lett.* **73** 1675; 1991 *Phys. Rev.* B **44** 9582; 1992 *Phys. Rev.* B **45** 5119(E)
[24] Tikofsky A M, Laughlin R B and Zou Z 1992 *Phys. Rev. Lett.* **69** 3670
[25] Shastry B S, Shraiman B I and Singh R R P 1993 *Phys. Rev. Lett.* **70** 2004
Deeg M, Fehske H and Büttner H 1994 *Europhys. Lett.* **26** 109
Dagotto E, Nazarenko A and Boninsegni M 1994 *Phys. Rev. Lett.* **73** 728
[26] Takagi H *et al* 1989 *Phys. Rev.* B **40** 2254
Hwang H Y *et al* 1994 *Phys. Rev. Lett.* **72** 2636